

Modeling Facial Soft Tissue Thickness for Automatic Skull-Face Overlay

B. Rosario Campomanes-Álvarez, Oscar Ibáñez, Carmen Campomanes-Álvarez,
Sergio Damas, and Oscar Cordón

Abstract—Craniofacial superimposition involves the process of overlaying a skull with a number of ante-mortem images of an individual and the analysis of their morphological correspondence. Within the craniofacial superimposition process, the skull-face overlay stage focuses on achieving the best possible overlay of the skull and a single ante-mortem image of a missing person. This technique has been commonly applied following a nonautomatic trial-and-error approach. Automatic skull-face overlay methods have been developed obtaining promising results. In this paper, we present two new variants that are an extension of existing 3-D-2-D methods to automatically superimpose a skull 3-D model on a facial photograph. We have modeled the imprecision related to the facial soft tissue depth between corresponding pairs of cranial and facial landmarks which typically guide the automatic approaches. As an illustration of the model's performance, the soft tissue distances associated to studies for Mediterranean population have been considered for dealing with this landmark matching uncertainty. Hence, we directly incorporate the corresponding landmark spatial relationships within the automatic skull-face overlay procedure. We have tested the performance of our proposal

Manuscript received January 9, 2015; revised April 16, 2015 and May 29, 2015; accepted May 30, 2015. Date of publication June 3, 2015; date of current version August 6, 2015. This work was supported in part by the Spanish Ministry of Economy and Competitiveness through the SOCOVIFI Project under Grant TIN2012-38525-C02-01/02, in part by the Juan de la Cierva Fellowship under Grant JCI-2012-15359, in part by the Principality of Asturias Government under Project CT13-55, in part by the Andalusian Department of Innovación, Ciencia y Empresa under Project TIC2011-7745, in part by the GENIL Programme through the CEI BioTic Granada under Project PYR-2014-14, in part by the Spanish MECD FPU under Grant AP-2012-4285, and in part by the European Union's Seventh Framework Programme for researching technological development and demonstration through the MEPROCS Project under Grant 285624, including European Development Regional Funds. The associate editor coordinating the review of this manuscript and approving it for publication was Prof. P. C. Yuen.

B. R. Campomanes-Álvarez and S. Damas are with the Department of Fuzzy Evolutionary Applications, European Centre for Soft Computing, Mieres 33600, Spain (e-mail: rosario.campomanes@softcomputing.es; sergio.damas@softcomputing.es).

O. Ibáñez is with the Department of Fuzzy Evolutionary Applications, European Centre for Soft Computing, Mieres 33600, Spain, and also with the Department of Computer Science and Artificial Intelligence, University of Granada, Granada 18014, Spain (e-mail: oscar.ibanez@decsai.ugr.es).

C. Campomanes-Álvarez is with the Department of Computer Science and Artificial Intelligence, University of Granada, Granada 18014, Spain (e-mail: carmen.campomanes@decsai.ugr.es).

O. Cordón is with the Department of Fuzzy Evolutionary Applications, European Centre for Soft Computing, Mieres 33600, Spain, also with the Department of Computer Science and Artificial Intelligence, University of Granada, Granada 18014, Spain, and also with the Research Center on Information and Communication Technologies, University of Granada, Granada 18014, Spain (e-mail: ocordon@decsai.ugr.es).

Color versions of one or more of the figures in this paper are available online at <http://ieeexplore.ieee.org>.

Digital Object Identifier 10.1109/TIFS.2015.2441000

on 18 skull-face overlay instances from a ground truth data set obtaining valuable results. The current proposal is thus the first automatic skull-face overlay method evaluated in a reliable and unbiased way.

Index Terms—Forensic anthropology, craniofacial identification, craniofacial superimposition, 3D-2D skull-face overlay, soft tissues, fuzzy sets and distances.

I. INTRODUCTION

THE techniques used to identify a missing person from skeletal information have been under continuous investigation within forensic anthropology [1], [2]. Craniofacial superimposition (CFS) [3], one of the approaches in craniofacial identification [4], [5], involves superimposing a skull onto a number of ante-mortem images of an individual and the analysis of their morphological correspondence.

Three consecutive stages for the whole CFS process have been distinguished in [6]: 1) Acquisition and processing of the skull and the ante-mortem facial photographs, together with the location of anatomical landmarks on the skull and the face; 2) Skull-face overlay (SFO), which focuses on achieving the best possible superimposition of a skull (or a skull 3D model) and a single ante-mortem image of a missing person. This process is iteratively repeated for each available photograph, obtaining different overlays. Skull-face overlay thus refers to what traditionally has been known as the adjustment of the skull size and its orientation with respect to the facial photograph [3]. It is the most time consuming stage of the whole CFS procedure. 3) Decision making where the degree of support shows that the skull and the available photograph belong to the same person or not (exclusion). This task requires a thorough analysis of the face/skull correspondence provided by SFO (second stage) to determine if the skull and the face actually belong to the same person. Currently, decision making in CFS must be manually taken by the human expert, a forensic anthropologist. This decision is guided by different criteria involving the relationship between the skull and the face: the morphological correlation, the matching between the corresponding landmarks according to the soft tissue depth and the consistency between asymmetries.

An important limitation of the CFS technique is the absence of a commonly accepted methodology.¹ Experts try to solve

¹There is a European project, entitled “New Methodologies and Protocols of Forensic Identification by Craniofacial Superimposition” (MEPROCS), which aims to develop a common methodology for the application of CFS. The interested reader is referred to <http://www.meprocs.eu/>.

the CFS problem by applying a specific strategy which uses their knowledge and the available technologies. During the SFO stage, the focus of this contribution, most forensic anthropologists follow a trial-and-error approach until they attain a good enough superimposition. The appropriate projection of the skull onto the facial photograph is a very challenging and time-consuming part of the CFS technique. This task involves the estimation of the best correspondence and it can take hours to arrive at the best possible fit [7], [8]. In addition, an inherent uncertainty exists because of overlaying two different “objects” (a skull and a face) [9]. Hence, a systematic and automatic SFO method is a real need in forensic anthropology [8].

Computational methods in the fields of computer vision (CV) and soft computing (SC) can be extremely useful of this proposal. Computer vision includes techniques for processing, analyzing, segmenting and registering image data in an automatic way [10]. Within CV, image registration (IR) aims to find a geometric transformation that overlays two images taken under different conditions (at different times, from different viewpoints, and/or by different sensors) [11]. Meanwhile, SC aims to design intelligent systems that process uncertain, imprecise and incomplete information [12]. Two of the main SC techniques are fuzzy logic (FL) [13] and evolutionary algorithms (EAs) [14]. The former extends classical logic to provide a conceptual framework of knowledge representation under imprecision and the consequent uncertainty. The latter combines powerful bio-inspired search and optimization tools to automate problem solving in areas such as modeling, simulation or global optimization [14]. Specifically, fuzzy sets have largely demonstrated their capability to deal with vagueness and imprecise information [13].

Our previous work tackles SFO automatically using EAs and fuzzy sets [9], [15]–[17]. These approaches are based on overlaying a skull 3D model on a facial photograph by minimizing the distance among pairs of landmarks as well as handling the imprecision due to the facial landmarks’ location [18], [19]. This minimization process involves the search for the specific projection of the skull 3D model that reduces all the distances between every pair of corresponding landmarks as much as possible. This is a good approximation to deal with the problem, which provides reasonable results but it is not anatomically correct. In fact, the anatomical distance between a cranial landmark and its corresponding facial point (soft tissue depth) is not considered. In reality, the thickness of the facial soft tissue differs for each corresponding pair of landmarks, varies among individuals and produces a mismatch among cranial and facial landmarks [5], [20]. Furthermore, another drawback of our proposals is that they have only been validated in a subjective way, based on the visual evaluation of the superimposition results by forensic experts. This is due to the lack of an objective assessment methodology in the area.

In this contribution, our proposal deals with the automation of the SFO task that is focused on the projection of a 3D skull model over a 2D photograph. We present an automatic 3D-2D SFO method which considers the imprecision related to the matching of landmarks in the skull and face. Thanks to fuzzy

sets [21], we have modeled the soft tissue thickness between pairs of cranial and facial landmarks. This novel proposal uses the same optimization mechanism employed before [9], [16] but it changes the formulation of the problem to directly incorporate the spatial relationships between corresponding landmarks. Unlike traditional SFO approaches locating tissue depth markers on the physical or the 3D model skull [20], [22], our proposal allows us to incorporate any soft tissue study easily.

In addition, we have performed an objective and quantitative evaluation of the SFO results. We included the soft tissue depth measurements of specific studies [23]–[25] within the SFO task. We tested the performance of our approach on 18 SFO problem instances that belong to the first and unique ground truth dataset [26]. This allows us to evaluate our automatic SFO method following an unbiased and reliable procedure. To our knowledge, the current proposal is the first automatic SFO procedure that incorporates forensic studies of inter-landmark distances and considers a ground truth dataset to validate the results.

The paper is organized as follows. Section II reviews the related work and the problem statement. Section III describes our proposals. Section IV presents the experiments and results. The discussion and conclusions are detailed in Section V.

II. BACKGROUND

A. Craniofacial Superimposition

Craniofacial superimposition [3] is one of the approaches in craniofacial identification [4], [5]. It involves the superimposition of a skull with a number of ante-mortem images of an individual and the analysis of their morphological correspondence. Since the first documented use of CFS for identification purposes [27], the technique has been under continuous improvement. Although the foundations of the CFS method were laid at the end of the nineteenth century [28], [29], the associated procedures evolved as new technology became available. Therefore, three different main approaches have been developed: photographic superimposition (developed in the mid 1930s), video superimposition (widely used since the second half of the 1970s) and computer-aided superimposition (introduced in the second half of the 1980s) [3], [4], [30].

The role of computerized systems in CFS is very important nowadays. Thus, special attention has been given to them in the more recent surveys in the field [6], [31]. In particular, they highlight the importance of stating the difference between non automatic and automatic computer-aided methods. Among the latter group, a reduced number of proposals deal with the same problem tackled in this manuscript: the SFO task. They obtain unbiased results and drastically reduce the time taken for SFO. These proposals are based either on photograph to photograph comparison [32] or on skull 3D model to photograph comparison [9], [15], [16], [30], [33].

B. Skull-Face Overlay as a Computer Vision Problem

Skull-face overlay requires positioning the skull in the same pose as the face in the photograph. From a purely CV point of view, the ante-mortem photograph is the result of the

2D projection of a real (3D) scene that was acquired by a particular (unknown) camera [34]. In such a scene, the living person was somewhere inside the camera's field of view in a given pose.

The most natural way to deal with the SFO problem is to replicate this original scenario. To do so, a 3D model of the skull must be used. Current 3D scanners provide skull 3D models with a precision of less than one millimeter in a few minutes [35]. These models can be properly handled using the computer, making the automation of the SFO task easier. Once the skull 3D model has been obtained, the goal is to adjust its size and its orientation with respect to the head in the photograph. In addition, the specific characteristics of the camera must also be replicated to reproduce the original situation as much as possible.

First, the skull 3D model is positioned in the camera coordinate system through geometric transformations, i.e., translation, rotation and scaling, which corresponds to the adjustment of the skull size and its orientation at the same angle as the face in the photograph [3], [7]. Then a perspective projection of the skull 3D model is placed onto the facial photograph.

Hence, a 3D-2D IR process where these unknown parameters are estimated seems to be the most appropriate formulation to automate SFO. In fact, that process directly replicates the original scenario in which the photograph was taken [15], [36].

C. Our Automatic Skull-Face Overlay Procedure

The 3D-2D IR approach is guided by the cranial and facial landmarks previously assigned by a forensic expert to the skull 3D model and the facial photograph.

Hence, given two sets of cranial and facial landmarks, $C = \{cl^1, \dots, cl^n\}$ and $F = \{fl^1, \dots, fl^n\}$, the process has to solve a system of equations with 12 unknowns [15]: the direction of the rotation axis $\vec{d} = (d_x, d_y, d_z)$, the location of the rotation axis with respect to the center of coordinates $\vec{r} = (r_x, r_y, r_z)$, the rotation angle θ , the factor s that scales the skull 3D model using the face in the photograph, the translation $\vec{t} = (t_x, t_y, t_z)$ that places the origin of the skull 3D model in front of the camera to replicate the moment of the photograph and the angle of view ϕ . These parameters determine the geometric transformation f that projects every cranial landmark cl^i of the skull 3D model onto its corresponding facial landmark fl^i of the photograph:

$$F = C \cdot R \cdot S \cdot T \cdot P \quad (1)$$

The rotation matrix R turns the skull to the same pose as the head in the photograph. S , T , and P are scaling, translation and perspective projection matrices respectively [15]. A complete description of the matrices of Eq. (1) is detailed in [37].

Using the cranial and facial landmarks, an EA iteratively searches for the best geometric transformation f , i.e., the optimal combination of the 12 parameters that minimizes the mean error (ME) fitness function [15]:

$$ME = \frac{\sum_{i=1}^N d(f(cl^i), fl^i)}{N}, \quad (2)$$

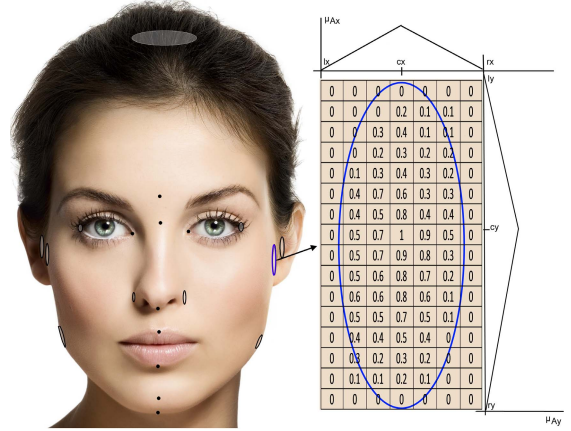


Fig. 1. Imprecise location of facial landmarks (left) and representation of a fuzzy landmark with fuzzy sets (right).

where cl^i is the 3D cranial landmark, fl^i is the 2D facial landmark, f is the geometric transformation, $f(cl^i)$ represents the 2D position of the 3D cranial landmark when projected onto the photograph, d is the 2D Euclidean distance, and N is the number of landmarks placed by the expert.

D. Modeling the Uncertainty Related to the Location of Facial Landmarks

The uncertainty related to the location of facial landmarks refers to the difficult task of placing landmarks on a photograph [18], [19]. Among other reasons, the definition of many anthropometric landmarks is imprecise in nature.

Using precise landmarks, forensic anthropologists can only place the facial landmarks that they clearly identify in the facial photograph. The fuzzy approach developed in [9] allows experts to enclose a region where the facial landmark is placed without any doubt by using variable-size ellipses (fuzzy landmarks) instead of locating a precise point as usual. The number of landmarks placed by the expert can thus increase when these landmarks are employed. This leads to a better description of the skull-face correspondence thanks to the new pairs of cranial points and fuzzy landmarks in the face. The performance of the automatic SFO method is thus improved.

As a consequence of handling these fuzzy landmarks, modeled as bi-dimensional fuzzy sets (see Fig. 1), the computation of the distances between the corresponding cranial and facial landmarks in Eq. 2 is affected as follows:

Distance from a point x to a fuzzy landmark \tilde{F} :

$$d'(x, \tilde{F}) = \frac{\sum_{k=1}^m d(x, \tilde{F}_k) \cdot \alpha_k}{\sum_{k=1}^m \alpha_k}, \quad (3)$$

where x is a precise point, \tilde{F}_k is the k th element (pixel) of the fuzzy landmark \tilde{F} , d is the 2D Euclidean distance, α_k is the membership value of \tilde{F}_k , and m is the number of elements of the fuzzy landmark \tilde{F} .

The interested reader is referred to [9] for a more in-depth explanation and an example of the calculation of the distance between a point and a fuzzy landmark.

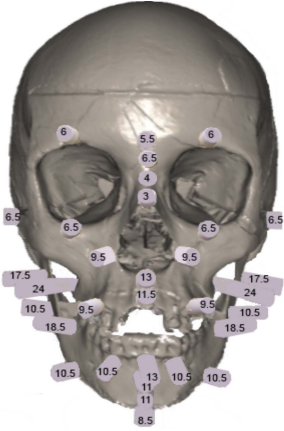


Fig. 2. Mean soft tissue depths (in mm) and spatial relationship between cranial and facial landmarks [23], [24].

Considering this latter distance (Eq. 3), the definition of the EA fitness function (Eq. 2) is modified as follows [9]:

$$\text{fuzzyME} = \frac{\sum_{i=1}^N d'(f(cl^i), \tilde{F}^i)}{N}, \quad (4)$$

where $f(cl^i)$ represents the 2D position of the 3D cranial landmark when projected onto the photograph, \tilde{F}^i represents the fuzzy landmark, and $d'(f(cl^i), \tilde{F}^i)$ is the distance between a point and a fuzzy landmark (Eq. 3), and the remaining parameters are those in Eq. 2.

III. INCORPORATING FACIAL SOFT TISSUE MODELING TO THE SKULL-FACE OVERLAY METHOD

Facial soft tissue depth varies for each landmark correspondence and for different groups of people. Some facial and cranial landmarks show a very close relationship as glabella, dacryon and frontotemporale. Meanwhile, others do not exactly overlap because of varying thicknesses in the soft tissue between them, e.g. gnathion, zygion and alare [20]. This variability has been widely studied in many populations and considering different age and gender subgroups [23], [24].

Our proposal goes beyond the use of tissue depth markers [22] as it directly incorporates the corresponding landmark spatial relationships and distances within the automatic SFO procedure (Fig. 2). To do this, we model the minimum (*min*), mean (*mean*) and maximum (*max*) distances between a pair of cranial and facial landmarks using fuzzy sets (what we defined as landmark matching uncertainty). These distances are obtained from any study looking at the specific population group considered.

In this section, we present two alternative approaches that deal with the landmark matching imprecision in SFO.

A. Modeling the Landmark Matching Uncertainty Using Spheres

Our first approach consists of building a fuzzy set whose center is the 3D cranial landmark with a membership degree of zero. The rest of the points are calculated adding the positive and negative values of the *min*, *mean* and *max*

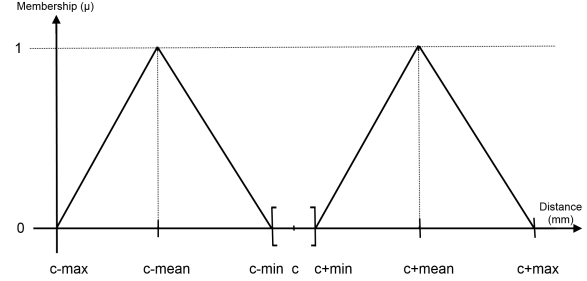


Fig. 3. Graphical representation of one of the dimensions of the 3D fuzzy set \tilde{B}_p for modeling the landmark matching uncertainty using a sphere. The other two dimensions are modeled in a homologous way.

distances to the 3D cranial landmark position along the three axes (X, Y and Z). We thus define a 3D volume (sphere) in the space where each facial landmark is expected to be located according to a particular soft tissue depth study (Figs. 2 and 4a).

We have chosen a triangular fuzzy set to define the masks for handling the landmark matching uncertainty. This choice is motivated by the large amount of literature available on the topic. Although different membership function shapes can be considered, both piece-wise (e.g. trapezoidal-shaped) and continuous (e.g. Gaussian), piece-wise triangular fuzzy membership functions are simpler and easier to handle. In addition, some works have proven that a linear piece-wise fuzzy membership function can approximate a continuous function to the desired degree, achieving similar results [38].

Formally, we handle the landmark matching uncertainty using 3D masks represented as a matrix M with $m_x \times m_y \times m_z$ points. These masks are defined by three triangular fuzzy sets \tilde{B}_x , \tilde{B}_y , and \tilde{B}_z , which model the approximate vertical, horizontal, and depth position of the sphere that represents the place of each facial landmark in relation with its cranial counterpart. They thus become 3D fuzzy sets, where each triangular fuzzy set \tilde{B}_p , with $p \in \{x, y, z\}$, is defined by its center $c \in \{c_x, c_y, c_z\}$ (the 3D coordinates of the cranial landmark) and the *min*, *mean*, and *max* distances as follows (see Fig. 3):

$$\tilde{B}_p = \begin{cases} 1 - \frac{|p - c + \text{mean}|}{\text{max} - \text{mean}}, & \text{if } c - \text{max} \leq p < c - \text{mean} \\ 1 - \frac{|p - c + \text{mean}|}{\text{mean} - \text{min}}, & \text{if } c - \text{mean} \leq p \leq c - \text{min} \\ 1 - \frac{|p - c - \text{mean}|}{\text{mean} - \text{min}}, & \text{if } c + \text{min} \leq p \leq c + \text{mean} \\ 1 - \frac{|p - c - \text{mean}|}{\text{max} - \text{mean}}, & \text{if } c + \text{mean} < p \leq c + \text{max} \\ 0, & \text{otherwise} \end{cases} \quad (5)$$

In the case that $p = x$, the point would be $c = c_x$. Hence, the calculated fuzzy set corresponds to \tilde{B}_x . If $p = y$ then $c = c_y$. Using this value, the defined fuzzy set is \tilde{B}_y . Finally, if $p = z$ implies that $c = c_z$. The resulting fuzzy set is \tilde{B}_z . The 3D fuzzy set \tilde{B}_{xyz} , which defines the whole sphere, is the result of applying the product t-norm of the latter three 1D fuzzy sets $\tilde{B}_{xyz} = \tilde{B}_x \cdot \tilde{B}_y \cdot \tilde{B}_z$. Its membership function is determined as $\mu_{\tilde{B}_{xyz}} = \mu_{\tilde{B}_x} \cdot \mu_{\tilde{B}_y} \cdot \mu_{\tilde{B}_z}$.

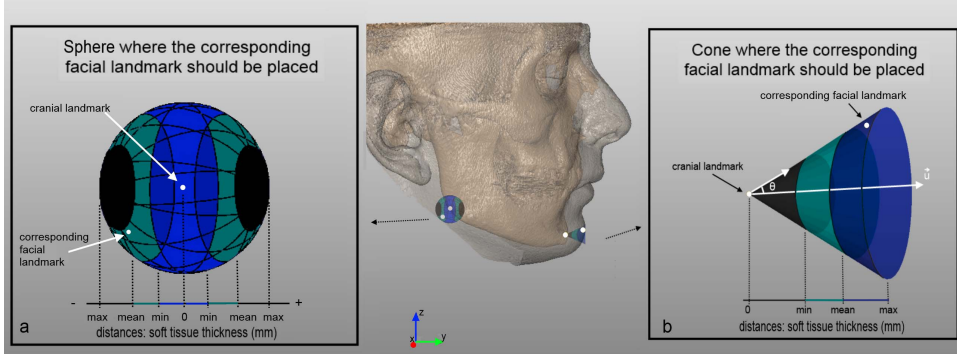


Fig. 4. Facial landmark position from a cranial landmark using a sphere (a) and a cone (b). *min*, *mean*, and *max* are the soft tissue depths. For the cone, \vec{u} is the normal vector at the cranial landmark in the skull, θ is the rotation angle of \vec{u} .

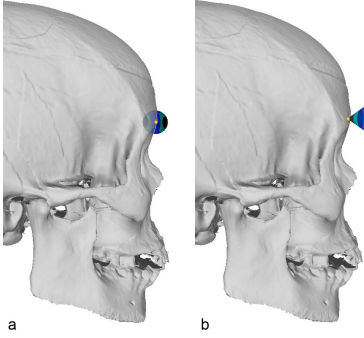


Fig. 5. Facial landmark position from a cranial landmark using a sphere (a) and a cone (b).

B. Modeling the Landmark Matching Uncertainty Using Cones

The previous approach is a good solution to tackle this SFO problem of modeling the facial soft tissue thickness with the available studies. However, it produces inconsistent anatomical solutions because it does not model the positional relationships between pairs of landmarks. For example, facial landmarks located inside the skull are considered to be correctly positioned (see the upper right part of the sphere in Fig. 4 and the whole left part of the sphere in Fig. 5a).

A variation of the previous method is proposed as follows: instead of modeling the soft tissue depth using a sphere with the cranial landmark in the center, we define a cone whose vertex is the cranial landmark. Each facial landmark is supposed to be located inside the cone (Fig. 4b). Using a cone, we closely specify a narrower region where the facial landmark should be located. We refine the search of the facial landmarks placement to a specific region. We assume a certain degree of perpendicularity between cranial and facial landmarks as most soft tissue studies do [23], [24].

To do this, we consider the normal vector² on the surface of the skull 3D model at each cranial landmark: $\vec{v} = (x_n, y_n, z_n)$. The unit vector of \vec{v} , which has the same direction,

but a magnitude of the unit, has been determined below:

$$\vec{u} = \left(\frac{x_n}{\|\vec{v}\|}, \frac{y_n}{\|\vec{v}\|}, \frac{z_n}{\|\vec{v}\|} \right) = (u_x, u_y, u_z), \quad (6)$$

where $\|\vec{v}\| = \sqrt{(x_n^2 + y_n^2 + z_n^2)}$ is the magnitude of \vec{v} .

In order to estimate the position of the facial landmarks, \vec{u} coordinates (u_x, u_y, u_z) are multiplied by the specific distance (*min*, *mean*, or *max*).

Since the correspondence between a pair of cranial-facial landmarks is not always perpendicular, different inclination angles are applied to the unit vector \vec{u} in order to define the volume in which the facial landmark is likely to be located. The amplitude of this area can be defined by a rotation equal to $\pm\theta$ along the three axes X, Y and Z.

The 3D rotation of the unit vector \vec{u} consists of three different rotations, i.e., a rotation of an angle $\pm\theta$ along the X, Y and Z axes [37]. The expressions for each axis rotation are the following:

$$X - axis \ rotation = \begin{cases} x' = u_x \\ y' = u_y \cdot \cos\theta - u_z \cdot \sin\theta \\ z' = -u_y \cdot \sin\theta + u_z \cdot \cos\theta \end{cases} \quad (7)$$

$$Y - axis \ rotation = \begin{cases} x' = u_x \cdot \cos\theta + u_z \cdot \sin\theta \\ y' = u_y \\ z' = -u_x \cdot \sin\theta + u_z \cdot \cos\theta \end{cases} \quad (8)$$

$$Z - axis \ rotation = \begin{cases} x' = u_x \cdot \cos\theta - u_y \cdot \sin\theta \\ y' = u_x \cdot \sin\theta + u_y \cdot \cos\theta \\ z' = u_z \end{cases} \quad (9)$$

Likewise, we define a fuzzy set whose center is the 3D cranial landmark with a membership degree of zero. The rest of the points are calculated by multiplying the coordinates of the unit vector \vec{u} by the values of the different distances *min*, *mean*, and *max*. Thus, a 3D cone is defined where each facial landmark is expected to be located according to a particular soft tissue depth study (Figs. 2 and 4b). The landmark matching uncertainty is defined using 3D masks in the same fashion as the spheres (see Sec. III.A). Hence, a fuzzy set \tilde{B}_p with $p \in \{x, y, z\}$ (see Fig. 6 for a graphical representation) is determined by its center $c \in \{c_x, c_y, c_z\}$ (the 3D coordinates of the cranial landmark), the normal vector

²The automatic and accurate estimation of a normal vector is not trivial in complex 3D surfaces with sharp regions and holes such as segmented CBCTs. Once estimated automatically, a forensic expert reoriented the normal vectors manually, if needed.

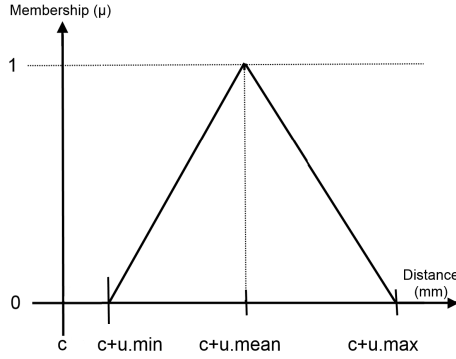


Fig. 6. Graphical representation of one of the dimensions of the 3D fuzzy set \tilde{B}_p for modeling the landmark matching uncertainty with a cone. The other two dimensions are modeled in a homologous way.

coordinates $u \in \{u_x, u_y, u_z\}$, and the *min*, *mean*, and *max* soft tissue distances:

$$\tilde{B}_p = \begin{cases} 1 - \frac{|p - c - u \cdot \text{mean}|}{u(\text{mean} - \text{min})}, & \text{if } c + u \cdot \min \leq p \leq c \\ & + u \cdot \text{mean} \\ 1 - \frac{|p - c - u \cdot \text{mean}|}{u(\text{max} - \text{mean})}, & \text{if } c + u \cdot \text{mean} < p \leq c \\ & + u \cdot \text{max} \\ 0, & \text{otherwise} \end{cases} \quad (10)$$

In the case that $p = x$, the points would be $c = c_x$ and $u = u_x$. Hence, the calculated fuzzy set corresponds to \tilde{B}_x . If $p = y$ then $c = c_y$ and $u = u_y$. Using these values, the defined fuzzy set is \tilde{B}_y . If $p = z$ it implies that $c = c_z$ and $u = u_z$, with the resulting fuzzy set being \tilde{B}_z .

The 3D fuzzy set \tilde{B}_{xyz} , which defines the whole 3D cone, is the product t-norm of the previous three, one-dimensional fuzzy sets $\tilde{B}_{xyz} = \tilde{B}_x \cdot \tilde{B}_y \cdot \tilde{B}_z$. Its membership function is determined by the product t-norm of the membership functions of each fuzzy set: $\mu_{\tilde{B}_{xyz}} = \mu_{\tilde{B}_x} \cdot \mu_{\tilde{B}_y} \cdot \mu_{\tilde{B}_z}$.

C. Distance Between Two Fuzzy Sets and Fitness Function Definition

Our proposal allows experts to mark both precise and imprecise (fuzzy) facial landmarks. These latter landmarks can be used by forensic anthropologists as necessary.

With the modeling of the landmark matching uncertainty proposed in the previous subsection, the need to compute the distance between two fuzzy sets arises. One of these two fuzzy sets is the projection of the 3D cranial landmark on the facial photograph, which is composed of the precise 3D cranial landmark (called cl^i in the two previous sections) and the fuzzy set that models the landmark matching uncertainty. The other fuzzy set would be the fuzzy facial landmark of the photograph representing the imprecise position of a facial landmark (Fig. 1).

The distance between two fuzzy sets \tilde{F} and \tilde{G} can be stated by [39]:

$$d''(\tilde{F}, \tilde{G}) = \frac{\sum_{k=1}^m \sum_{l=1}^n (d(\tilde{F}_k, \tilde{G}_l) \cdot \min[\alpha_k, \beta_l])}{\sum_{k=1}^m \sum_{l=1}^n \min[\alpha_k, \beta_l]}, \quad (11)$$

where \tilde{F}_k is the k_{th} element of the fuzzy set \tilde{F} , \tilde{G}_l is the l_{th} element of the fuzzy set \tilde{G} , d is the 2D Euclidean distance, α_k is the membership value of \tilde{F}_k , β_l is the membership value of \tilde{G}_l , m is the number of elements of the fuzzy set \tilde{F} , and n is the number of elements of the fuzzy set \tilde{G} .

Therefore, the fitness function *Fuzzy Mean Error* (FME) for the current automatic 3D-2D SFO task has been formulated by taking into account the latter fuzzy distances:

$$FME = \frac{\sum_{i=1}^{N_{\text{crisp}}} (d'(x_i, f(\tilde{C}^i)) + \sum_{j=1}^{N_{\text{fuzzy}}} (d''(\tilde{F}^j, f(\tilde{C}^j)))}{N}, \quad (12)$$

where N_{crisp} is the number of 2D facial landmarks precisely located (crisp points), N_{fuzzy} is the number of 2D facial landmarks imprecisely located and defined as bi-dimensional fuzzy sets, N is the total number of landmarks considered ($N = N_{\text{crisp}} + N_{\text{fuzzy}}$), x_i corresponds to a 2D facial landmark defined as a crisp point ($x_i \in F$), \tilde{C}^i and \tilde{C}^j are fuzzy sets modeling each 3D cranial landmark and the soft tissue distance to the corresponding 3D facial landmark i or j ; f is the function that determines the 3D-2D perspective transformation that properly projects every 3D skull point onto the 2D photograph (Eq. 1); $f(\tilde{C}^i)$ and $f(\tilde{C}^j)$ are two fuzzy sets, corresponding to the result of applying the perspective transformation f to the 3D volume (either sphere or cone), which model the landmark matching uncertainty; \tilde{F}^j represents the fuzzy set of points of the imprecise 2D facial landmark; $d'(x_i, f(\tilde{C}^i))$ is the distance between a point and a fuzzy set of points, and $d''(\tilde{F}^j, f(\tilde{C}^j))$ is the distance between two fuzzy sets.

Solving the SFO problem results in an extremely complex optimization task with a highly *multimodal* landscape. This scenario led us to face the problem of considering robust EAs to search for the optimal values of the 12 registration transformation parameters, as discussed in Sec. II.C.

IV. EXPERIMENTS

Some detailed experiments have been developed to analyze the performance of our approaches, including the treatment of the landmark matching uncertainty in comparison with the state-of-the-art SFO automatic methods proposed in [9] and [16], which do not consider this capability.

A. Materials

The experimental design involves 18 SFO problem instances corresponding to nine cases of live people (from Spain and Italy) that will allow the study of ground truth data and the subsequent objective evaluation. These instances

were created as follows [26]: The subjects were submitted to cone-beam computed tomography (CBCT) for clinical purposes. It generates precise 3D models (0.3 mm slices) in an orthostatic position and it thus avoids undesired gravitational effects on the soft tissue.

During the same clinical session, two digital photographs were taken in frontal and lateral poses. The patients were in an orthostatic position and asked to maintain a neutral expression. Unfortunately, CBCTs only scan from the lowest part of the mandible to the eyebrows without including the top of the head (see Fig. 4). The photographs were taken at a distance of between 1 m and 1.5 m, using a digital camera with a minimum resolution of 4 Mpx.

The images resulting from the CBCT device were automatically processed to obtain the 3D models of both the skull and the face. After positioning homologous points on the facial 3D model and its corresponding photograph, the former was automatically projected onto the latter using a geometric transformation g so they perfectly matched, i.e., an actual 3D face - 2D face overlay. Then, this geometric transformation g was applied to project the skull 3D model onto the photograph resulting in a perfect SFO. The latter is considered as the ground truth projection of the skull onto the facial photograph that can later be compared with the outcome of every SFO method. As a result, we obtained the ground truth data which is the 2D coordinates of the 3D cranial landmarks projected onto the photograph by means of g .

The skull 3D models and the facial photographs were stored using the Face2SkullTM software [40], which has been developed by our team. This software allows forensic experts to precisely position the cranial landmarks as well as place the facial landmarks on the photographs in a precise and imprecise (using ellipses) manner. Face2SkullTM also integrates and runs the proposed automatic SFO algorithms. All the experiments have been performed on an Intel CoreTM 2 Quad CPU Q8400 2.66 GHz, with 4GB RAM, running Windows 7 ProfessionalTM.

B. Experimental Design

First, we compared the performance of the state-of-the-art automatic approaches RCGA and CCGA-2 [9], [16], neither of which model the landmark matching uncertainty. These proposals calculate the distance between a skull and its corresponding facial landmark by means of the fitness function defined in Eq. (4). We developed this experiment because the previous proposals had not tested using a ground truth dataset. Furthermore, they were compared only with imprecise metrics in six SFO problem instances corresponding to three cases [16]. The parameter configuration used for testing these approaches is that which obtained the best results in [15] and [16] respectively. The EA with the best performance was chosen to incorporate the facial soft tissue.

In the next step, we included triangular membership functions in the best EA of the previous analysis, to model the facial soft tissue following the two new proposals based on spheres and cones.

Furthermore, the influence of the fuzzy membership function type was analyzed using the method that showed the

TABLE I
MEAN ERROR IN mm REGARDING THE GROUND TRUTH OBTAINED
IN 30 RUNS FOR EACH CASE, COMPARING CCGA-2 WITH RCGA.
 $f =$ FRONTAL AND $l =$ LATERAL POSES OF THE FACE IN THE
PHOTOGRAPH, $pl =$ NUMBER OF PRECISE LANDMARKS
AND $pi =$ NUMBER OF IMPRECISE LANDMARKS
LOCATED BY THE EXPERTS IN EACH CASE

Case, pose	pl	il	CCGA-2	RCGA
1,f	7	7	4.565	2.750
1,l	5	4	16.588	7.406
2,f	8	5	4.906	3.690
2,l	3	2	8.299	8.605
3,f	8	7	3.815	3.629
3,l	4	4	9.367	10.643
4,f	7	6	4.635	3.647
4,l	4	3	14.027	14.327
5,f	10	6	2.996	2.436
5,l	5	4	8.545	6.865
6,f	8	7	4.654	3.784
6,l	3	4	16.486	12.959
7,f	10	5	4.253	3.639
7,l	5	4	10.212	12.663
8,f	9	6	5.269	4.409
8,l	4	4	6.840	8.555
9,f	10	4	6.174	5.541
9,l	3	5	10.210	11.701
Average (mm)			7.778	6.976

best performance in the experiment. The two other most common fuzzy membership functions (piece-wise trapezoidal and Gaussian) were tested.

Finally, to better understand the behavior of our proposal, we have included a study based on negative cases. We tested the best algorithm, i.e., RCGA-c-45 using a triangular fuzzy set function when a 3D skull and a photograph belong to different persons.

Since all these methods are based on stochastic processes, 30 independent runs were performed for each problem instance to compare the robustness of the methods and to avoid any possible bias.

C. Performance Analysis of the Existing CCGA-2 and RCGA Approaches

Table I presents the mean error achieved for each case and pose ($f =$ frontal view and $l =$ lateral view) by RCGA and CCGA-2 in the 30 runs performed as well as the total average error per algorithm.

The distance error has been calculated for all the landmarks marked in each case study. The mean error of a case study refers to the average of all their single landmark errors. The total average error corresponds to the average of all mean errors of a particular algorithm.

As a result of the comparison between RCGA and CCGA-2, RCGA achieved the best behavior in 13 of the 18 cases with

TABLE II
MEAN ERROR IN mm REGARDING THE GROUND TRUTH OBTAINED
IN 30 RUNS FOR EACH CASE USING DIFFERENT
PARAMETRIZATION FOR RCGA, f = FRONTAL
AND l = LATERAL POSES OF THE FACE
IN THE PHOTOGRAPH

Case, pose	RCGA s	RCGA c-0	RCGA c-10	RCGA c-30	RCGA c-45
1,f	2.727	4.116	4.330	3.078	3.164
1,l	6.938	7.400	6.693	5.788	5.828
2,f	3.486	3.823	4.212	3.337	3.331
2,l	8.871	8.871	8.871	5.286	3.688
3,f	3.664	6.594	6.594	3.007	2.941
3,l	10.815	11.073	11.073	7.604	7.001
4,f	3.505	3.356	3.356	3.223	3.045
4,l	13.494	13.847	13.847	12.446	12.171
5,f	2.453	2.204	2.406	2.641	2.600
5,l	6.097	6.846	6.846	3.715	2.825
6,f	3.644	2.618	3.076	2.878	2.921
6,l	11.665	2.204	11.126	11.009	10.626
7,f	3.617	4.695	4.695	4.100	3.714
7,l	10.909	9.649	9.649	9.729	10.345
8,f	3.579	3.492	3.492	2.856	2.882
8,l	7.812	19.935	19.935	6.262	5.412
9,f	5.757	6.660	6.660	5.071	4.887
9,l	11.700	19.852	19.852	10.391	9.509
Average (mm)	6.548	7.759	8.416	5.585	5.281

significant differences in most of them. Thus, we selected RCGA to incorporate the facial soft tissue modeling.

D. Performance Analysis of the New Proposals Incorporating the Facial Soft Tissue Modeling

We call the new proposals RCGA-s and RCGA-c. RCGA-s corresponds to the approach that deals with the landmark matching uncertainty using spheres. In the case of RCGA-c, the landmark matching uncertainty is modeled with cones. Within RCGA-c, four different angles were tested to define the cone amplitude: $\theta = \pm 0^\circ$, $\theta = \pm 10^\circ$, $\theta = \pm 30^\circ$, and $\theta = \pm 45^\circ$, so we analyzed four variants of this proposal: RCCA-c-0, RCGA-c-10, RCGA-c-30 and RCGA-c-45. They both use the fitness function defined in Eq. (12). The experiment again consisted of 30 independent runs for each problem instance.

The best performance regarding the ground truth is obtained by RCGA-c-45 in most of the cases (see Table II). In frontal views, RCGA-c-0 obtains the most accurate results for cases 5 and 6, RCGA-s for case 1, and RCGA-c-45 for the rest of the cases. The mean error of the best cases ranges from 2.204 to 4.887 mm. In lateral views, the most precise SFOs correspond to RCGA-c-45 and RCGA-c-0 or cases 4 and 5, while RCGA-c-45 obtains the best results in all instances except cases 1 (RCGA-c-30)

and 7 (RCGA-c-0 and RCGA-c-10). The best mean errors are higher than in the frontal view, it achieves values between 2.204 and 9.649 mm.

RCGA-c-45 and RCGA-c-30 achieve a total average error of 5.281 and 5.585 mm respectively. RCGA-s gives more than 6 mm of total average error: 6.548 mm, and the worse algorithm is RCGA-c-10 with 8.416 mm (Table II).

Figure 7a, c shows the best superimpositions obtained for the two photographs of the fifth case as a particular illustration of the methods' performance. These outcomes have been achieved by RCGA-c-0 and RCGA-c-45 for the frontal and the lateral image respectively. In particular, blue points (dark gray in the black and white version of this manuscript) refer to the cranial landmarks after overlaying the skull 3D model onto the photograph. Yellow points (light gray in the black and white version) are the actual landmarks achieved by the ground truth geometric transformation g . Green points (gray in the black and white version) are the facial landmarks marked by the expert in the photograph. We should remind readers that these facial points have been placed as either precise or imprecise (ellipses) landmarks. Each ellipse contains a gray point corresponding to its center. For better visualization, the resulting matching between pairs of cranial and ground truth landmarks for case 5 (frontal and lateral view) are depicted in Fig. 7b, d.

RCGA-c-0 obtains the most accurate solution regarding the ground truth in the frontal image, with a total average error of 2.204 mm (Table II). The two gonions present a larger distance with respect to their counterpart ground truth points (Fig. 7a, b). In the case of the lateral pose, the best overlay has been achieved by RCGA-c-45 with an error equal to 2.825 mm. Alare right and subnasale are the closest points to their corresponding ground truth landmarks (Fig. 7c, d).

Figure 7e and g presents the SFOs in frontal and lateral views for case 5, achieved by the best algorithm without incorporating the modeling of the landmark matching uncertainty (RCGA). The resulting matching between pairs of cranial and ground truth landmarks are depicted in Fig. 7f, h. RCGA obtains the larger error in the two ectocanthions, the two endocanthions, nasion, gonion right, alare and zygion left for the frontal image (Fig. 7e, f). The mean total error of RCGA is 2.436 mm for the frontal photograph in case 5 (Table I). In the lateral image, RCGA-c-10 presents a higher error in all landmarks compared with RCGA-c-45 (Fig. 7d, h). We can also see that the skull protrudes from the face in the nasal region (Fig. 7g). A manual refinement would be needed for this SFO result. The mean total error of RCGA in the lateral view is 6.865 mm (Table I).

In general, we obtained competitive matchings between pairs of corresponding cranial and facial landmarks in all the studied cases. As previously noted, the best results are obtained by the new proposals, which include the treatment of the landmark matching uncertainty.

We performed a Friedman test [41] to analyze whether significant differences exist among the performance of all the approaches. The aim was to test a null hypothesis stating that the mean total errors of all the approaches were the same. We set the experiment level of significance at $\alpha = 0.05$.

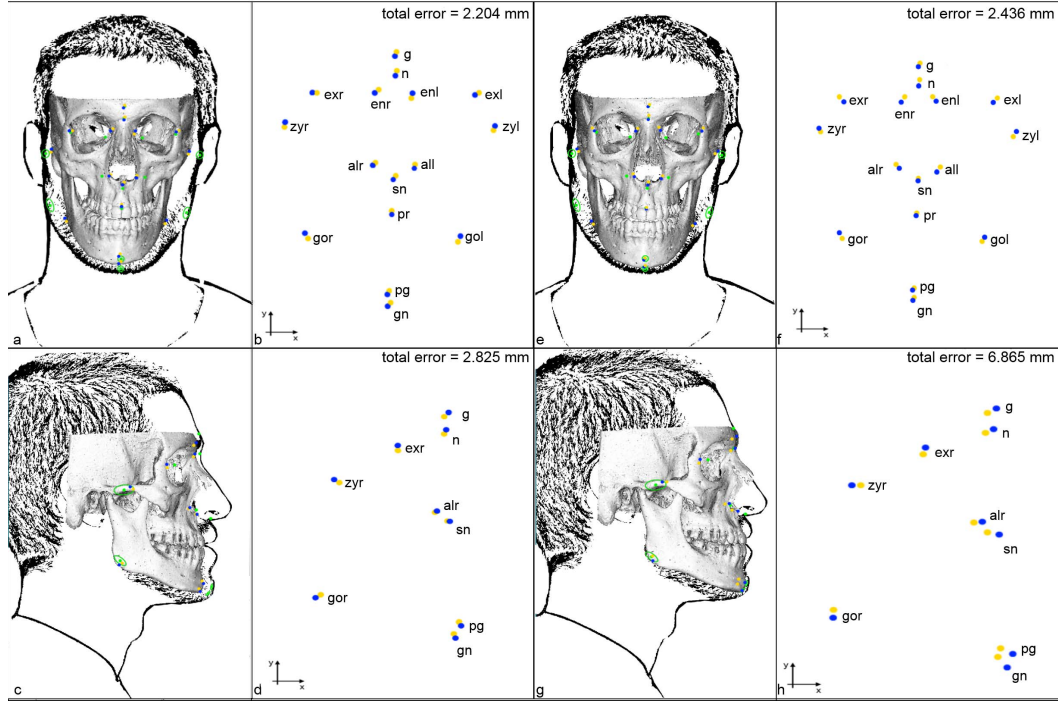


Fig. 7. Case 5. Best (a, c) and RCGA (e, g) automatic SFOs for frontal and lateral poses. Best (b, d) and RCGA (f, h) matching between pairs of projected cranial and actual ground truth landmarks for frontal and lateral views. Frontal images: glabella (g), nasion (n), exocanthion left, right (exl, exr), endocanthion left, right (enl, enr), alare left, right (all, alr), subnasale (sn) and prostion (pr) were marked as precise facial landmarks. Zygion left, right (zyl, zyr), gonion left, right (gol, gor), pogonion (pg) and gnathion (gn) were placed as imprecise facial landmarks. Lateral images: Glabella (g), nasion (n), exocanthion right (exr), alare right (alr) and subnasale (sn) were placed in the photograph as a precise points. Zygion right (zyr), pogonion (pg) and gnathion (gn) were marked as imprecise facial landmarks. The homologous cranial landmarks were placed on the skull as precise points.

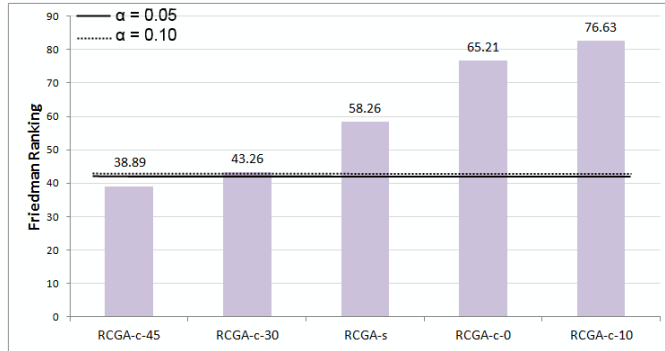


Fig. 8. Friedman ranking and Bonferroni-Dunn lines for the classification rate.

The statistic results of this test are a Friedman χ^2 equal to 43.9695 and a p value of 7.496e-08. This data reveals significant differences among the behavior of the approaches with a p value < 0.0001 , thus rejecting the null hypothesis. Due to the rejection of the null hypothesis, a post-hoc statistical analysis is needed. A Bonferroni-Dunn test [42] was carried out to detect significant differences among a control approach and the rest. RCGA-c-45 was the control algorithm because it outperformed the remaining methods, i.e., it obtained the lowest value in the Friedman ranking (Fig. 8). In the Bonferroni-Dunn test, we obtain 3.093 and 2.856 as critical values using levels of significance $\alpha = 0.05$ and $\alpha = 0.10$ respectively.

Figure 8 summarizes the ranking obtained by the Friedman test. The bar height indicates the average ranking of

TABLE III
p VALUES FOR THE COMPARISON BETWEEN THE CONTROL
AND THE REST OF THE APPROACHES

Approach	Unadjusted p	p Bonf	p Holm
(RCGA-c-45 is the control)			
RCGA-s	0.0502	1.0000	0.5531
RCGA-c-0	0.0003	0.0077	0.0063
RCGA-c-10	<0.0001	0.0003	0.0003
RCGA-c-30	0.6216	1.0000	1.0000

each proposal. We draw a line through the chart whose value is the sum of the smallest bar height (the best approach) and the critical value achieved by the Bonferroni-Dunn test. Bars which are higher than the line are the methods whose performance is significantly worse than the control approach [43].

We also applied a paired t test with a Bonferroni and a Holm correction, as well as an unadjusted p value in order to learn the differences within approaches [44].

Table III details the pairwise comparisons considering RCGA-c-45 as the control approach. The p value is indicated in each comparison and we have marked in bold the approaches which are worse than the control, considering a level of significance at $\alpha = 0.05$.

RCGA-c-45 statistically outperforms the rest of the approaches with a confidence level of 95% except for RCGA-s and RCGA-c-30 (Table III). These results corroborate the data obtained by the Bonferroni-Dunn test applied to the Friedman

TABLE IV
MEAN ERROR IN mm REGARDING THE GROUND TRUTH OBTAINED
IN 30 RUNS FOR EACH CASE, USING DIFFERENT FUZZY
MEMBERSHIP FUNCTIONS FOR THE BEST ALGORITHM
RCGA-c-45, f = FRONTAL AND l = LATERAL
FACIAL POSES IN THE PHOTOGRAPH

Case, pose	RCGA-c-45	RCGA-c-45	RCGA-c-45
		Gaussian	trapezoidal
1,f	3.164	2.960	3.052
1,l	5.828	6.116	5.465
2,f	3.331	3.071	3.165
2,l	3.688	4.436	4.618
3,f	2.941	2.774	2.816
3,l	7.001	7.487	7.325
4,f	3.045	3.102	3.105
4,l	12.171	11.875	10.747
5,f	2.600	2.527	2.524
5,l	2.825	3.451	3.158
6,f	2.921	3.058	2.979
6,l	10.626	10.900	11.692
7,f	3.714	3.653	3.679
7,l	10.345	10.821	10.279
8,f	2.882	2.908	2.896
8,l	5.142	6.693	6.680
9,f	4.887	5.164	5.200
9,l	9.509	9.575	9.626
Average (mm)	5.281	5.490	5.406

ranking where RCGA-c-45 and RCGA-c-30 present a better behavior than the other approaches (Fig. 8).

E. Analysis of the Influence of the Fuzzy Membership Function Type on the Landmark Matching Uncertainty Modeling

In order to finish studying the optimal design for our innovative approach, we analyzed the performance of the best automatic SFO method (RCGA-c-45) when considering two other types of fuzzy membership functions: piece-wise trapezoidal and Gaussian. Table IV presents the mean error obtained in each case and pose in the 30 runs performed for the new analyzed approaches, as well as the total average error per algorithm regarding the ground truth dataset.

The best performance is again obtained by RCGA-c-45 using a triangular fuzzy set function (total average = 5.281 mm). RCGA-c-45 with a Gaussian fuzzy set function is the best algorithm in cases 2 and 3 for frontal view. In lateral view cases 1 and 4, RCGA-c-45 with a trapezoidal function gives the best results.

We also performed a Friedman test [41] following the previous experiment design. The aim was to test a null hypothesis stating that the mean total errors of all the methods are the same. We set the experiment level of significance at $\alpha = 0.05$. The statistic results are a Friedman χ^2 equal

to 63.336 and a p value of 73.244e-11, thus rejecting the null hypothesis. A Bonferroni-Dunn test was performed due to the rejection of the null hypothesis using RCGA-c-45 triangular fuzzy function as the control algorithm. We obtained 3.330 and 3.106 as critical values using a level of confidence $\alpha = 0.05$ and $\alpha = 0.10$ respectively.

We also applied a paired t test with a Bonferroni and a Holm correction, as well as an unadjusted p value to discover the differences between approaches, considering RCGA-c-45 with a triangular fuzzy set function as the control approach. This analysis reveals that no significant difference is obtained between RCGA-c-45 (triangular membership function) and RCGA-c-45-Gaussian. Likewise, no significant difference is achieved between the RCGA-c-45 and RCGA-c-45-trapezoidal methods.

Therefore, we cannot assert that modeling the soft tissue depth between corresponding pairs of cranial and facial landmarks using trapezoidal and Gaussian fuzzy functions is significantly better than using triangular fuzzy functions for RCGA-c-45. Due to the fact that triangular fuzzy functions are quicker to handle, easier to implement and obtain the best total error regarding the ground truth (Table IV), we have chosen this type of function to model the uncertainty related to the soft tissue depth between pairs of cranial and facial landmarks.

F. Negative Cases Study

In this final experiment the goal was two-fold. On the one hand, to show the behavior of our proposal using unrelated skull 3D models and facial photographs. On the other hand, to make clear that the aim of our method is to obtain the best possible SFO, without assuming any particular skull-face relationship *a priori*, rather than addressing the third CFS stage, i.e., the decision making.

Thus, our best algorithm was run over the same data set employed before (distinguishing between female and male cases) but this time superimposing each skull 3D model over the frontal and lateral images of the remaining subjects (i.e., each SFO involves a 3D skull and a photograph not belonging to the same person). We considered RCGA-c-45 using a triangular fuzzy set function and the same parameter set as in the previous experiments.

Tables V and VI present the fuzzy mean errors for the female and male negative cases respectively. Notice that the fuzzy mean error we used to evaluate each SFO within the EA-IR process is a measure of the quality of the overlay but cannot be used to directly determine if the skull and the face actually belong to the same person. In fact, as depicted in Tables V and VI, this error is smaller for some negative cases in comparison with their positive counterparts (for example, the skull in the first case with the frontal and lateral images of case 3, the skull in case 2 with the lateral images of cases 3 and 8, etc.). This simple experimentation allows us to illustrate that the purpose of our approach is to try to achieve the best possible skull-face overlay without assuming any particular skull-face correspondence. Decision making, carried out by forensic anthropologists, is a different and also challenging task where they have to consider different criteria

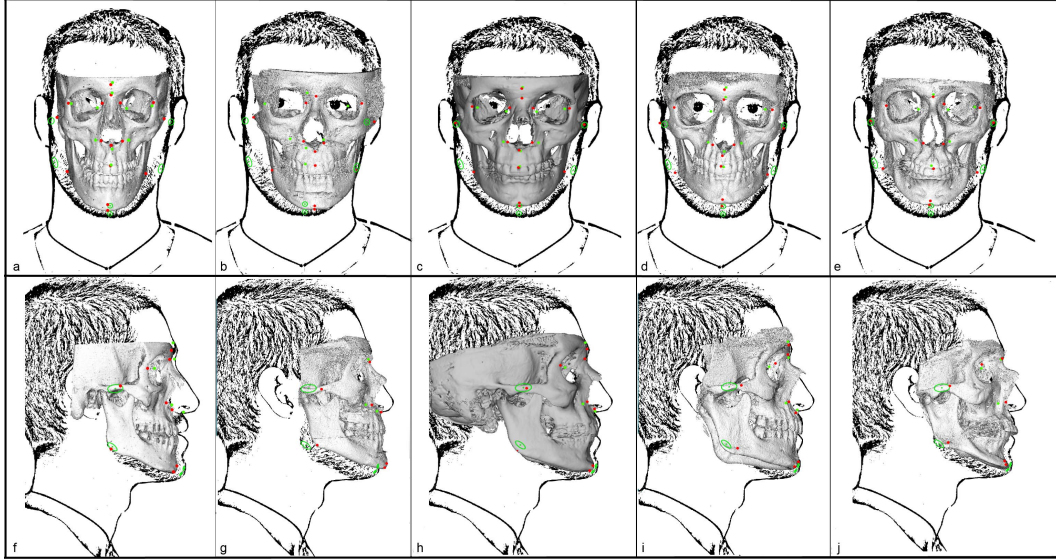


Fig. 9. Skull-face overlays achieved by the best algorithm RCGA-c-45 using the photographs (frontal and lateral poses) of case 5. (a) and (f) frontal and lateral SFOs (respectively) using the actual skull (positive case). From (b) to (e): SFOs using the frontal image of case 5 and the skulls of cases 4, 6, 7 and 9 respectively (negative cases). From (g) to (j) SFOs using the lateral image of case 5 and the skulls of cases 4, 6, 7 and 9 respectively.

TABLE V

FUZZY MEAN ERROR (FME) IN PIXELS OBTAINED IN 30 RUNS FOR ALL THE FEMALE CASES USING THE BEST ALGORITHM RCGA-c-45,
 $f = \text{FRONTAL}$ AND $l = \text{LATERAL}$ FACIAL POSES IN THE
 PHOTOGRAPH. POSITIVE CASES ARE HIGHLIGHTED
 IN BOLD, THE REST ARE NEGATIVE ONES

Image,pose \ Skull	1	2	3	8
1,f	0.020	0.060	0.040	0.066
1,l	0.022	0.057	0.049	0.059
2,f	0.027	0.061	0.039	0.061
2,l	0.028	0.047	0.040	0.060
3,f	0.015	0.055	0.034	0.045
3,l	0.016	0.021	0.034	0.034
8,f	0.025	0.056	0.039	0.047
8,l	0.030	0.039	0.040	0.045

such as analyzing the consistency of the bony and facial outlines/morphological curves, assessing anatomical consistency by positional relationship, marking and comparing lines to analyze anatomical consistency and evaluating the consistency of the soft tissue thickness among corresponding cranial and facial landmarks [3].

In order to illustrate the results of our proposal when dealing with negative cases, Fig. 9 shows the best superimpositions obtained by the RCGA-c-45 algorithm for the negative cases corresponding to the case 5 photographs (frontal and lateral poses) and the 3D skull of the male cases 4, 6, 7 and 9. The obtained overlays for the positive cases considering the actual subject of the fifth skull have also been included for comparison. Red points (dark gray in the black and white version of this manuscript) refer to the cranial landmarks after overlaying the skull 3D model on the photograph.

TABLE VI

FUZZY MEAN ERROR (FME) IN PIXELS OBTAINED IN 30 RUNS FOR ALL THE MALE CASES USING THE BEST ALGORITHM RCGA-c-45,
 $f = \text{FRONTAL}$ AND $l = \text{LATERAL}$ FACIAL POSES IN THE
 PHOTOGRAPH. POSITIVE CASES ARE HIGHLIGHTED
 IN BOLD, THE REST ARE NEGATIVE ONES

Image,pose \ Skull	4	5	6	7	9
4,f	0.035	0.074	0.049	0.039	0.072
4,l	0.035	0.076	0.028	0.039	0.076
5,f	0.080	0.043	0.049	0.049	0.050
5,l	0.048	0.034	0.020	0.049	0.054
6,f	0.046	0.073	0.027	0.045	0.069
6,l	0.019	0.049	0.023	0.059	0.082
7,f	0.051	0.079	0.050	0.034	0.073
7,l	0.020	0.050	0.028	0.051	0.084
9,f	0.048	0.076	0.050	0.049	0.047
9,l	0.003	0.050	0.029	0.058	0.058

Green points (light gray in the black and white version) are the facial landmarks marked by the forensic anthropologist in the photograph.

In particular, the fuzzy mean error of the lateral positive case number 5 is 0.034 while the error of the negative case using skull 6 and the image of case 5 is 0.020 (see Table VI). However, Fig. 9h shows that the latter negative superimposition is not correct because the nasal bone protrudes from the face, which can be quickly detected by an expert.

V. DISCUSSION AND CONCLUSIONS

The SFO process is a repetitive and tedious task in CFS. It requires several hours to overlay a skull on a facial photograph. The design of unbiased, systematic, automatic and

quantifiable methods to perform SFO is a real need in forensic anthropology [8].

Within CFS, we have just focused on the SFO stage. The main goal of our methodology is to assist forensic anthropologists to obtain the best possible overlay, i.e., orienting and positioning the skull on the facial photograph, reducing the SFO processing time and simplifying their work.

Our method is aimed at automating the SFO task, the most time consuming one involving the projection of a skull model over a face picture. During the last century, this procedure has been tackled by manual or semi-automatic methods based on the use of either skull photographs (skull-photo superimposition) or a video mixing device (video superimposition). Recently, forensic anthropologists have determined that the use of a 3D skull model is a more informative representation, but the manual projection has remained. Our proposal involves the design of an automatic method to obtain accurate 3D skull-2D face overlays in a short time by considering the imprecision related to the matching of landmarks in the skull and face. However, the human identification decision, considered as the final output, is taken in the third stage, decision making. This decision is manually taken by a forensic anthropologist, applying her/his knowledge and expertise to analyze the skull-face overlay obtained as the output of the second CFS stage. In addition, notice that the fuzzy mean error we defined to deal with SFO in the second stage is a measure of the quality of the skull-face overlay but cannot be used to directly determine if the skull and the face actually belong to the same person. Forensic anthropologists consider different criteria to take their final decision.

The correspondence between facial and cranial landmarks is not always symmetrical and perpendicular. We have defined two proposals to deal with this source of uncertainty by using fuzzy sets and taking into account the available information concerning soft tissue depths. In particular, we have considered the measurements of the facial soft tissue distances detailed in two studies for Mediterranean populations [23]–[25].

We have chosen a triangular fuzzy set by defining the masks for handling the landmark matching uncertainty related to the facial soft tissue distances. This choice is motivated by the large amount of literature available on the topic. Although different membership function shapes can be considered, both piece-wise (e.g. trapezoidal-shaped) and continuous (e.g. Gaussian), piece-wise triangular fuzzy membership functions are simpler and easier to handle, providing a quicker response. In addition, some works have proven that a linear piece-wise fuzzy membership function can approximate a continuous function to the desired degree, achieving similar results [38].

The performance of our automatic approaches and the two previous ones [9], [16], which do not include the landmark matching uncertainty treatment, have been objectively evaluated considering a ground truth dataset in 18 case studies. Our proposals achieve a competitive matching between pairs of corresponding cranial and facial landmarks because of the natural modeling of the landmark correspondences using SC techniques. In particular, RCGA-c-45 significantly outperforms the remaining automatic SFO methods tested. It obtains

the best performance regarding the ground truth in the majority of the cases. The RCGA-c-30 variant also achieves a good ranking in the computed statistical analysis (in fact, it is the same method with a different parametrization). Hence, the new proposals that model the landmark matching uncertainty get better results than the previous approaches that do not consider the facial soft tissue thickness.

In order to extend our experiment, we analyzed the performance of the best automatic SFO method (RCGA-c-45) when considering another two types of fuzzy membership function: piece-wise trapezoidal and Gaussian, which model the soft tissue depth between pairs of corresponding cranial and facial landmarks. The performance of the SFO method considering these two kinds of membership functions was compared with the rest of the methods previously implemented (either based on the use of triangular fuzzy sets to model the soft tissue depth or not taking into account the soft tissue depths). The best performance is also obtained by RCGA-c-45 using a triangular fuzzy set function. RCGA-c-45 with Gaussian and trapezoidal fuzzy set functions achieve good results. However, statistical analysis shows that modeling the soft tissue depth between corresponding pairs of cranial and facial landmarks using RCGA-c-45 with trapezoidal and Gaussian fuzzy functions is not significantly better than using RCGA-c-45 with triangular fuzzy functions. Furthermore, to better understand the behavior of our proposal, we have included a study based on negative cases. We have tested the best algorithm, i.e., RCGA-c-45 using a triangular fuzzy set function when a 3D skull and a photograph belong to different people. The fuzzy mean errors of negative cases are lower than the fuzzy mean error in the positive ones. This shows the proper behavior of our proposal, which only searches for the best possible SFO.

Although valuable results are obtained, it is important to note that a distance or residual error is still obtained when evaluating an SFO result against its corresponding ground truth overlay. A few sources of uncertainty (imprecision) are behind these errors. We list them together with possible solutions that could serve as future lines of research to improve SFO accuracy:

Our method makes use of soft tissue studies which provide population-based mean and standard deviation distances for corresponding landmarks. We neither consider the real cranial and facial landmark distances of each individual nor their exact spatial orientation (as would be the case in a real-world scenario when faced the identification of an unknown skull). This error could be mitigated having more information about the skull-face relationships. In particular, it could be extremely useful to measure the spatial orientations of the facial landmarks with respect to their corresponding cranial points in order to model the landmark matching uncertainty accordingly.

Our approach relies on the location of cranial and facial landmarks. As has already been explained in this article, placing landmarks on a photograph is a difficult task that presents a particular degree of imprecision [18], [19]. Thus, the imprecision in the location of landmarks has a negative effect on the final SFO achieved (best transformation). This problem could be minimized either including a final refinement

stage relying only on these landmarks that are known to be more precisely located [18], [19] and/or guiding the overlay algorithm not only with landmarks but also with corresponding anatomical regions, i.e., teeth overlapping.

Finally, in our proposal we are trying to overlay a rigid 3D model (the whole skull) onto a photograph of the person where the underlying bony part is not rigid, i.e., the mandible in the photograph could have a different articulation than in the skull 3D model. To address this source of error, the mandible in the 3D model could be manually or automatically articulated accordingly to its position in the photograph. Note that this source of error could be considered insignificant in our study since all the patients were asked to have the same facial gesture while scanning and photographing [26].

REFERENCES

- [1] K. R. Burns, *Forensic Anthropology Training Manual*, 3rd ed. Upper Saddle River, NJ, USA: Pearson Education, 2012.
- [2] C. Cattaneo, "Forensic anthropology: Developments of a classical discipline in the new millennium," *Forensic Sci. Int.*, vol. 165, nos. 2–3, pp. 185–193, 2007.
- [3] M. Yoshino, "Craniofacial superimposition," in *Craniofacial Identification*, C. Wilkinson and C. Rynn, Eds. Cambridge, U.K.: Cambridge Univ. Press, 2012, pp. 238–253.
- [4] W. A. Aulsebrook, M. Y. İşcan, J. M. Slabbert, and P. Becker, "Superimposition and reconstruction in forensic facial identification: A survey," *Forensic Sci. Int.*, vol. 75, pp. 101–120, Oct. 1995.
- [5] C. N. Stephan, "Craniofacial identification: Techniques of facial approximation and craniofacial superimposition," in *Handbook of Forensic Anthropology and Archaeology*, vol. 25, S. Blau and D. Ubelaker, Eds. Walnut Creek, CA, USA: Left Coast Press, 2009, pp. 304–321.
- [6] S. Damas *et al.*, "Forensic identification by computer-aided craniofacial superimposition: A survey," *ACM Comput. Surv.*, vol. 43, no. 4, 2011, Art. ID 27.
- [7] T. W. Fenton, A. N. Heard, and N. J. Sauer, "Skull-photo superimposition and border deaths: Identification through exclusion and the failure to exclude," *J. Forensic Sci.*, vol. 53, no. 1, pp. 34–40, 2008.
- [8] D. H. Ubelaker, "A history of Smithsonian–FBI collaboration in forensic anthropology, especially in regard to facial imagery [abstract]," *Forensic Sci. Commun.*, vol. 2, no. 4, 2000.
- [9] O. Ibáñez, O. Cordón, S. Damas, and J. Santamaría, "Modeling the skull-face overlay uncertainty using fuzzy sets," *IEEE Trans. Fuzzy Syst.*, vol. 19, no. 5, pp. 946–959, Oct. 2011.
- [10] M. Sonka, V. Hlavac, and R. Boyle, *Image Processing, Analysis, and Machine Vision*, 3rd ed. Toronto, ON, Canada: Thomson-Engineering, 2007.
- [11] B. Zitová and J. Flusser, "Image registration methods: A survey," *Image Vis. Comput.*, vol. 21, pp. 977–1000, Oct. 2003.
- [12] P. P. Bonissone, "Soft computing: The convergence of emerging reasoning technologies," *Soft Comput.*, vol. 1, no. 1, pp. 6–18, 1997.
- [13] L. A. Zadeh, "Soft computing and fuzzy logic," *IEEE Softw.*, vol. 11, no. 6, pp. 48–56, Nov. 1994.
- [14] A. Eiben and J. E. Smith, *Introduction to Evolutionary Computing*. Heidelberg, Germany: Springer-Verlag, 2003.
- [15] O. Ibáñez, L. Ballerini, O. Cordón, S. Damas, and J. Santamaría, "An experimental study on the applicability of evolutionary algorithms to craniofacial superimposition in forensic identification," *Inf. Sci.*, vol. 179, no. 23, pp. 3998–4028, 2009.
- [16] O. Ibáñez, O. Cordón, and S. Damas, "A cooperative coevolutionary approach dealing with the skull-face overlay uncertainty in forensic identification by craniofacial superimposition," *Soft Comput.*, vol. 18, no. 5, pp. 797–808, 2012.
- [17] O. Ibáñez, O. Cordón, S. Damas, and J. Santamaría, "An advanced scatter search design for skull-face overlay in craniofacial superimposition," *Expert Syst. Appl.*, vol. 39, no. 1, pp. 1459–1473, 2012.
- [18] M. Cummaudo *et al.*, "Pitfalls at the root of facial assessment on photographs: A quantitative study of accuracy in positioning facial landmarks," *Int. J. Legal Med.*, vol. 127, no. 3, pp. 699–706, 2013.
- [19] B. R. Campomanes-Álvarez, O. Ibáñez, F. Navarro, I. Alemán, O. Cordón, and S. Damas, "Dispersion assessment in the location of facial landmarks on photographs," *Int. J. Legal Med.*, vol. 129, no. 1, pp. 227–236, 2015.
- [20] G. M. Gordon and M. Steyn, "An investigation into the accuracy and reliability of skull-photo superimposition in a South African sample," *Forensic Sci. Int.*, vol. 216, pp. 198.e1–198.e6, Mar. 2012.
- [21] L. A. Zadeh, *Fuzzy Sets, Fuzzy Logic, and Fuzzy Systems*. Singapore: World Scientific, 1996.
- [22] C. G. Birngruber, K. Kreutz, F. Ramsthaler, J. Krähahn, and M. A. Verhoff, "Superimposition technique for skull identification with Afloat software," *Int. J. Legal Med.*, vol. 124, no. 5, pp. 471–475, 2010.
- [23] C. N. Stephan and E. K. Simpson, "Facial soft tissue depths in craniofacial identification (part I): An analytical review of the published adult data," *J. Forensic Sci.*, vol. 53, no. 6, pp. 1257–1272, 2008.
- [24] C. N. Stephan and E. K. Simpson, "Facial soft tissue depths in craniofacial identification (part II): An analytical review of the published sub-adult data," *J. Forensic Sci.*, vol. 53, no. 6, pp. 1273–1279, 2008.
- [25] L. Valencia-Caballero, "Metodología para elaborar reconstrucciones faciales empleando gráficos computarizados tridimensionales," (in Spanish), Ph.D. dissertation, Lab. Antropología Forense, Univ. Granada, Spain, 2007.
- [26] O. Ibáñez, F. Cavalli, B. R. Campomanes-Álvarez, C. Campomanes-Álvarez, A. Valsecchi, and M. I. Huete, "Ground truth data generation for skull-face overlay," *Int. J. Legal Med.*, vol. 129, no. 3, pp. 569–581, 2015.
- [27] J. Glaister and J. C. Brash, *The Medico-Legal Aspects of the Ruxton Case*. Edinburgh, TX, USA: Harcourt Brace/Churchill Livingstone, 1937.
- [28] F. Galton, *The Bertillon System of Identification* (Review of Signaletic Instructions, Alphonse Bertillon), vol. 54. Chicago, IL, USA: McClaughry RW, 1896, pp. 569–570.
- [29] P. Broca, *Instructions craniologiques et craniométriques de la Société d'Anthropologie de Paris*, (in French), vol. 6. Paris, France: Bulletin de la Société d'Anthropologie, 1875, pp. 534–536.
- [30] B. A. Nickerson, P. A. Fitzhorn, S. K. Koch, and M. Charney, "A methodology for near-optimal computational superimposition of two-dimensional digital facial photographs and three-dimensional cranial surface meshes," *J. Forensic Sci.*, vol. 36, no. 2, pp. 480–500, 1991.
- [31] M. I. Huete, T. Kahana, and O. Ibáñez, "Past, present, and future of craniofacial superimposition: Literature and international surveys," *Int. J. Legal Med.*, 2015, doi: 10.1016/j.legalmed.2015.02.001.
- [32] A. K. Ghosh and P. Sinha, "An economised craniofacial identification system," *Forensic Sci. Int.*, vol. 117, pp. 109–119, Mar. 2001.
- [33] W. Jin, G. Geng, K. Li, and Y. Han, "Parameter estimation for perspective projection based on camera calibration in skull-face overlay," in *Proc. Int. Conf. Virtual Reality Vis. (ICVRV)*, Sep. 2013, pp. 317–320.
- [34] O. Faugeras, *Three-Dimensional Computer Vision: A Geometric Viewpoint*. Cambridge, MA, USA: MIT Press, 1993.
- [35] H.-K. Park, J.-W. Chung, and H.-S. Kho, "Use of hand-held laser scanning in the assessment of craniometry," *Forensic Sci. Int.*, vol. 160, pp. 200–206, Jul. 2006.
- [36] B. R. Campomanes-Álvarez *et al.*, "Computer vision and soft computing for automatic skull-face overlay in craniofacial superimposition," *Forensic Sci. Int.*, vol. 245, pp. 77–86, Dec. 2014.
- [37] D. Hearn and M. P. Baker, *Computer Graphics, C Version*. Upper Saddle River, NJ, USA: Prentice-Hall, 1997.
- [38] M. Delgado, M. A. Vila, and W. Voxman, "On a canonical representation of fuzzy numbers," *Fuzzy Sets Syst.*, vol. 93, no. 1, pp. 125–135, 1998.
- [39] I. Bloch, "On fuzzy distances and their use in image processing under imprecision," *Pattern Recognit.*, vol. 32, no. 11, pp. 1873–1895, 1999.
- [40] Face2skull™ Software. [Online]. Available: <http://www.face2skull.com/>, accessed Jun. 15, 2015.
- [41] M. Friedman, "A comparison of alternative tests of significance for the problem of m rankings," *Ann. Math. Statist.*, vol. 11, no. 1, pp. 86–92, 1940.
- [42] O. J. Dunn, "Multiple comparisons among means," *J. Amer. Statist. Assoc.*, vol. 56, no. 293, pp. 52–64, 1961.
- [43] S. García, A. Fernández, J. Luengo, and F. Herrera, "A study of statistical techniques and performance measures for genetics-based machine learning: Accuracy and interpretability," *Soft Comput.*, vol. 13, no. 10, pp. 959–977, 2009.
- [44] S. P. Wright, "Adjusted p-values for simultaneous inference," *Biometrics*, vol. 48, no. 4, pp. 1005–1013, 1992.



B. Rosario Campomanes-Álvarez received the Ph.D. degree in computer science from the University of Oviedo, Spain, in 2015. She is currently a Postdoctoral Researcher with the European Centre for Soft Computing, Spain. Her main research interests include soft computing, computer vision, and forensic identification.



Sergio Damas received the Ph.D. degree in computer science from the University of Granada, Spain. Since 2011, he has been a Principal Researcher of Fuzzy-Evolutionary Applications with the European Centre for Soft Computing, Spain. His current research interests are in the fields of soft computing for forensic anthropology and medical imaging, fuzzy logic, computer vision, evolutionary computation, and their applications to different real-world problems.



Oscar Ibáñez received the Ph.D. degree in computer science from the University of Santiago de Compostela, Spain, in 2010. He is currently a Postdoctoral Researcher with the University of Granada. His research interests include evolutionary computation, fuzzy logic, computer vision, machine learning, and their applications to tackle real-world problems with a particular interest in forensic identification.



Carmen Campomanes-Álvarez received the M.S. degrees in telecommunication engineering and information technologies and communications in mobile networks from the University of Oviedo, Spain, in 2011 and 2012, respectively. She is currently pursuing the Ph.D. degree in information and communications technologies with the University of Granada, Spain. Her research interests are focused on forensic identification using soft computing.



Oscar Cordón received the Ph.D. degree in computer science from the University of Granada, Spain, in 1997. He is currently a Full Professor with the Department of Computer Science and Artificial Intelligence, University of Granada. He is an Associate Editor of 11 international journals and a Reviewer of more than 40 journals. His current main research interests are in the fields of soft computing for forensic anthropology and medical imaging, fuzzy rule-based systems and genetic fuzzy systems, evolutionary computation, ant colony optimization and other single and multi-objective metaheuristics, and their applications to different real-world problems.